

GTD for Ground Screens with Rounded Tops

Draft Oct 31, 2017, L. Page

The geometric theory of diffraction (GTD) was developed to enable reasonable diffraction calculations for objects of most any shape. We often use it to compute the power diffracted from the ground and into our receivers. It can also be used to compute the sidelobes of a uniformly illuminated aperture. There is an example in Page et al. Fig. 3. [6].

The purpose of this note is to compute the power diffracted into the Small Aperture Camera (SAC) for the Simons Array but I hope the note is more generally useful. To go beyond the classic Sommerfeld solution is involved but worth pursuing.

The executive summary is 1) Make sure the ground screen has a rounded top with radius of curvature ~ 10 cm. 2) The diffracted radiation will be vertically polarized. 3) For a ground screen whose top has a 10 cm radius and is 5 m away at an angle of 30° , the effective temperature of radiation entering an aperture is $20 \mu\text{K}$ at 150 GHz and $80 \mu\text{K}$ at 90 GHz. This is still $\sim 10^3$ greater than the signal we are after. The last figure in this memo shows the design parameter space.

1 Geometry and basic equations

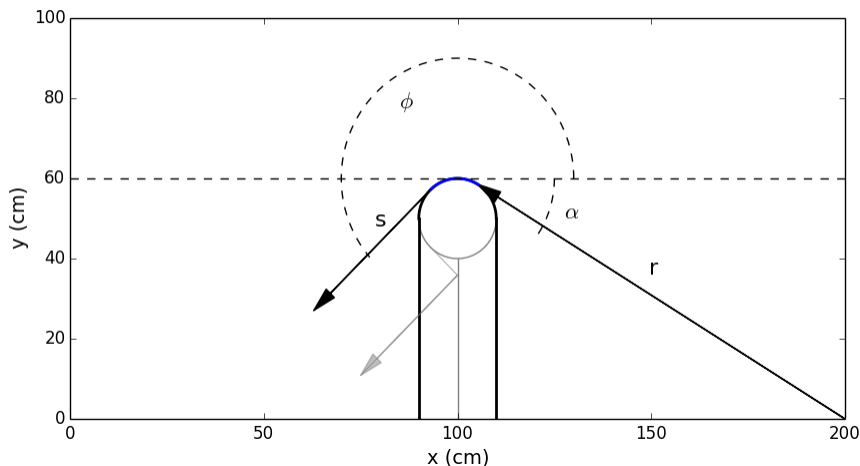


Figure 1: The geometry and coordinates for diffraction from a rounded screen. The coordinates s and r are measured from their tangent points on the cylinder. The angles are determined with respect to the horizontal. Here $\phi = 225^\circ$ and $\alpha = 31.7^\circ$. In this note we take α positive as drawn. Keller treats the case where $\alpha = 0$. The blue region shows the area where the ray diffracts around the cylinder. For most of the results presented in this note, the bottom grey ray may be ignored.

We work in cylindrical coordinates following Keller[2, 3, 4]. Figure 1 shows the geometry we will use. Sommerfeld showed that for knife edge diffraction over the top of a half plane

the diffracted field is

$$u_d = u_s \frac{e^{i(ks+\pi/4)}}{\sqrt{s}} \left[\frac{e^{i\pi}}{2\sqrt{2\pi k}} \left(\frac{1}{\cos[(\phi + \alpha)/2]} \pm \frac{1}{\sin[(\phi - \alpha)/2]} \right) \right] = u_s \frac{e^{i(ks+\pi/4)} e^{i\pi}}{\sqrt{ks}} f_s(\phi, \alpha). \quad (1)$$

Here u_s is the field on the knife edge and u_d is the diffracted field a distance s from the edge. These may be thought of as electric fields. In cylindrical geometry the power drops off like $1/r$. In this expression, the “+” corresponds to the boundary condition $u = 0$ on the screen which corresponds to the electric field being parallel to the edge of the screen. The “-” sign corresponds to $\partial u/\partial n = 0$ or the electric field being perpendicular to the edge of the ground screen. The wavevector is $k = 2\pi/\lambda$. The solution is valid for $kr \gg 1$ which will always be the case for us. It is not applicable close to $\phi + \alpha = \pi$. The expression inside the large square brackets is the diffraction coefficient, D . We’ll find that it is easier to work with the dimensionless quantity $\sqrt{k}D = f_s(\phi, \alpha)$ which is the diffraction pattern scattered from the edge. The appearance of \sqrt{k} is from the implicit Fourier transform that is part of any diffraction problem. The solution can be found in many texts. My favorite is Born and Wolf [1]. The convention is to call α as drawn negative. We will take it as positive; equation 1 is adjusted accordingly.

The full treatment of the problem is given in Levy and Keller [5]. They start their rays at some point p away from the cylinder so that the incident field (u_s in Equation 1) becomes

$$u_i = u_p e^{i\pi/2} \frac{e^{i(kr-\pi/4)}}{2\sqrt{2\pi kr}}. \quad (2)$$

The overall normalization is discussed below. Note that the diffracted field in equation 1 looks just like the above, up to $e^{i\pi}$, but with the field multiplied by a geometric factor. Now in reality the edges have some finite radius of curvature a . Equation 1 is for $a=0$. We want the solution for some finite a . This is worked out in general in Levy and Keller in a language that does not easily translate to what we want to compute or to [3]. One goal of this note is to translate that paper into something we can use.

For one ray, the solid one in Figure 1, which is all we need to consider,

$$u_d = u_i \frac{e^{i(ks-\pi/2)}}{\sqrt{sk}} \sum_m \sqrt{k} D_m^2 e^{(ik-\alpha_m)t} \quad (3)$$

where the D_m^2 are the diffraction coefficients and the α_m are the attenuation coefficients for the field traveling a distance t over the curved surface. This equation is general and applies to any ray from the source to the receiver. The sum is over the multiple modes for one ray that propagates over the curved edge. The thing Levy and Keller did was to posit the above form and compare it to rigorous solutions in cylindrical and spherical geometries to determine the D_m and the α_m . The calculations are quite involved and general. They are summarized in the following table which is adapted from Table 1 in [5].

In general there will be multiple rays diffracting around some object and we just sum up the fields from each of them. For these applications it is important to keep track of the phase because the waves interfere. For the ground screen there is just one ray which makes

Table 1: GTD Diffraction and attenuation coefficients

Case	Boundary Condition	$\alpha_m = e^{-i\pi/6} \left(\frac{k}{6a^2}\right)^{1/3} q_m$
I	$u = 0$	$A_G(q_m) = 0$
II	$\partial u/\partial n = 0$	$A'_G(q_m) = 0$
IV	$\partial u/\partial n$ continuous	$\frac{A'_G(q_m)}{A_G(q_m)} = e^{i5\pi/6} \left(\frac{ka}{6}\right)^{1/3} \left[\left(\frac{k_1}{k}\right)^2 - 1\right]^{1/2} \frac{b}{b_1}$
Case	Boundary Condition	$k^{1/2} D_m^2$
I	$u = 0$	$e^{i5\pi/4} (2\pi)^{1/2} \frac{\pi e^{i5\pi/6}}{6} \left(\frac{ka}{6}\right)^{1/3} \frac{1}{[A'_G(q_m)]^2}$
II	$\partial u/\partial n = 0$	$e^{i5\pi/4} (2\pi)^{1/2} \frac{\pi e^{i5\pi/6}}{2} \left(\frac{ka}{6}\right)^{1/3} \frac{1}{q_m [A_G(q_m)]^2}$
IV	$\partial u/\partial n$ continuous	$e^{i5\pi/4} (2\pi)^{1/2} \frac{\pi e^{i5\pi/6}}{6} \left(\frac{ka}{6}\right)^{1/3} \frac{1}{[A'_G(q_m)]^2 + (q_m [A_G(q_m)]^2)/3}$

the problem relatively straight forward. From the form of the equations, it is clear that this is a scalar theory. The full vector aspects of E&M are not incorporated.

So how does this work? Referring to the solution presented in Table 1, we'll consider the boundary conditions $u = 0$ on the surface (Case I) and $\partial u/\partial n = 0$ on the surface (Case II) and come back to Case IV later ($\partial u/\partial n$ is continuous). We don't need to consider their Case III. First we need to find the q_m . These are obtained by finding the roots of the Airy function and its derivatives, A_G and A'_G . One of the subtleties of the calculation is that Levy and Keller do not use the standard definition of the Airy function. Their definition is related to the standard one (e.g., Scipy) by

$$A_G(x) = \pi 3^{-1/3} A(-3^{-1/3}x) \quad \text{and} \quad A'_G(x) = -\pi 3^{-2/3} A'(-3^{-1/3}x). \quad (4)$$

In Cases I and II one just needs to compute the roots once and then you are set. Their examples are based on just the first root which for many cases is all that's needed.

Table 2: Roots of the Keller Airy function and its derivative

Root m	q_m for $A_G = 0$	$A'_G(q_m)$	q_m for $A'_G = 0$	$A_G(q_m)$
Root m	$u = 0$	$u = 0$	$\partial u/\partial n = 0$	$\partial u/\partial n = 0$
0	3.37213	-1.05905	1.46935	1.166799
1	5.89584	1.21296	4.68471	-0.91272
2	7.96202	-1.30674	6.95179	0.82862
3	9.78813	1.37568	8.88903	-0.77962
4	11.45742	-1.43078	10.63252	0.74562
5	13.01291	1.47698	12.24252	-0.71986
6	14.48043	-1.51692	13.75250	0.69927
7	15.87704	1.55221	15.18351	-0.68220

In Cases I and II there is no loss due to the finite conductivity to the surface over which the ray is propagating. The rounded edge is effective because diffracted energy peels off as the ray propagates over the surface. Once the roots are obtained, it is straight forward to compute the α_m and D_m^2 to compute the field.

Cases III and IV include the loss in energy in the ray from propagating over the surface. Here the root is complex, depends on the material, and on the radius of curvature. For good conductors, the properties are:

$$\epsilon = 1 + \frac{i\sigma}{\epsilon_0\omega} \quad \text{and} \quad k_1 = \epsilon^{1/2}\frac{\omega}{c} \quad (5)$$

where $\epsilon_0 = 8.854 \times 10^{-12}$ F/m is the dielectric constant of space in SI units. For aluminum, $\sigma = 3.5 \times 10^7$ S/m and so at 150 GHz the index is $n = 1448 + i1448$. The wavevector $k = 3140 \text{ m}^{-1}$ in free space or $k_1 = 4.549 \times 10^6(1+i) \text{ m}^{-1}$ in aluminum. The quantities $b = k^2/\mu$ and $b_1b = k_1^2/\mu_1$ are set by boundary conditions. Because $k_1 \gg k$, the right hand side in the equation for $A'_G(q_m)/A_G(q_m)$ in Table 1 is small and the problem essentially reduces to that of finding the roots of $A'_G(q_m) = 0$. This is not too surprising because aluminum is a good conductor and the equations were worked out assuming a perfect conductor. To summarize, *the diffracted ray depends on geometry; the resistive loss from traveling over the material is negligible.*

2 Example: Diffraction over a rounded edge

Keller [3] asks the question ‘‘How dark is the Shadow of Round-Ended Screen?’’ The geometry is shown in Figure 1. He takes $\alpha = 0^\circ$ and gives his results for $\phi = 225^\circ$. He considers two cases. The one applicable for us is when the ray diffracts over the top and into a detector. In this case, the ray travels 45° on the surface. The second is when the screen is round on top but has the ray go through 135° then bounce off the vertical wall that holds the rounded end. The ray emerges parallel to the one that just went through 45° and interferes with it. The geometry for this is shown in grey.

The ray diffracting over the rounded top is a good example to consider because it shows how the theory works. Unfortunately it is not clear how one generalizes from what Keller presents. Our goal is to consider more general cases. In the shadow, the field is given by

$$u_d = u_i \frac{e^{i(ks+\pi/4)}}{\sqrt{ks}} \left[(ka)^{1/3} \frac{C_0}{\sqrt{2}} e^{-i\pi/6} e^{i(ka+\tau_0(ka)^{1/3})\theta_s} \right] = u_i \frac{e^{i(ks+\pi/4)}}{\sqrt{ks}} f(\theta_s, ka). \quad (6)$$

where $\theta_s = 45^\circ$ is the angle the ray travels over the screen. After going through these calculations it became clear that one gets a good approximation of the effect of a rounded edge if one uses Keller’s equation with $\theta_s = \phi + \alpha$ where ϕ and α are the angles in Sommerfeld’s formula. More rigorously, comparing to the above, we find

$$\tau_0 = -\frac{q_0}{6^{1/3}} e^{-i\pi/6} e^{-i\pi/2} \quad \text{and} \quad C_0 = \frac{\sqrt{2k}}{(ka)^{1/3}} e^{i\pi/12} D_0^2. \quad (7)$$

In his work, Keller treats C_0 as real and in effect always takes the absolute value¹. More generally we find

$$f(\theta_s, ka) = \sum_m D_m'^2 e^{(ika - \alpha'_m)\theta_s}, \quad (8)$$

where $D_m'^2 = \sqrt{k} D_m^2$ and $\alpha'_m = a\alpha_m$

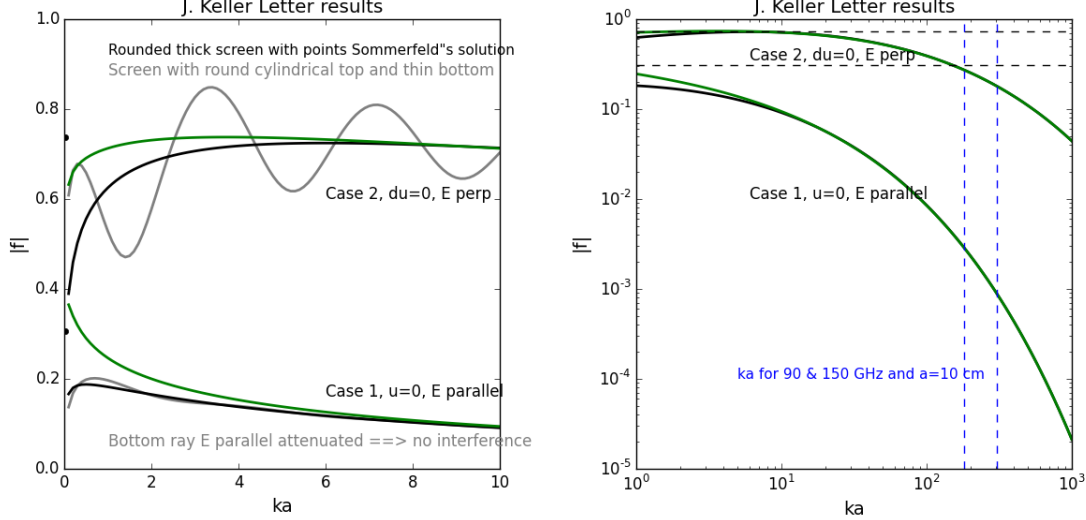


Figure 2: *Left:* Results for the Keller example. The solid black lines are for the round-ended ground screen with one term in the mode expansion. These match the plots in [3]. The green lines are the same case but now including 8 terms in the mode expansion. Note that for $ka > 6$ there is no need to include higher modes. The dots on the left axis are the Sommerfeld solution with Case II on top. The grey lines are for the more complicated path with a bounce, interference with the grey arrow in Figure 1. These also match Keller's solution. *Right:* The same plot but for an expanded range in ka . Again this shows that the higher modes are not needed. The two vertical blue lines are for $ka = 182$ and 303 corresponding to 87 and 145 GHz with a radius of curvature of $a=10$ cm. The horizontal dashed lines are the Sommerfeld solution again with Case II on top. Note that the diffracted radiation is vertically polarized and that rounding the top of the ground screen can have a large effect. At $ka = 303$ the ratio of the rounded edge case to the Sommerfeld case is $0.18/0.74 = 0.24$ for the vertical polarization, or 6% in power. A plot of the results for Case IV overlaps that of Case II.

In Figure 2 we show that our calculation reduces to Keller's plot. Keller didn't go beyond q_0 but we can. The bottom line is that for $ka > 6$ one needs only the 0^{th} root. The higher order terms bring the GTD solution closer to the exact solution but never quite reach it.

¹In [5] there is a pernicious typo on page 188. They have $A_G(q_0) = 1.668$ whereas it should be $A_G(q_0) = 1.1668$. The ratio is close to $3^{1/3}$ which complicated understanding the Airy function normalization.

3 The input field from the ground

The normalization of the input field can be confusing and I have oscillated within a factor of two on what it should be. I think the following is correct but would like to hear others thoughts.

Let's say we have an electric field on the ground of strength $\mathcal{E}_g = \eta T_g^{1/2}$. A distance r away in cylindrical coordinates, the electric field will have the *rms* value $E = \eta T_g^{1/2}/r^{1/2}$. From this we can compute the power emitted from a differential area element on the ground of size dA from $\int S dA = \int c\epsilon_0 E^2 dA$. At some point above the ground, this has to be the power flowing through a small little rectangle of size $c\epsilon_0 u^2 \Delta z \Delta h$. This means the incident field is $u_i = \eta T_g^{1/2}/\sqrt{\Delta h}$. Here Δh can be thought of as the "height" of the ray. Of course the field does not go to infinity as Δh gets small but in GTD we need to transform the input flux to an electric field represented by a ray. This construction allows us to accomplish that.

The ground is a Lambertian emitter. That is, the total power from a given dA is multiplied by $\cos(\psi)$ where ψ is the angle to the normal. Integrating over this factor reduces the diffracted power by a factor of two. From Figure 1, $\psi = \pi/2 - \alpha$ and so $\cos(\psi) = \sin(\alpha)$. It follows that the total power from dA is $dS = c\epsilon_0 E^2 \sin \alpha dA$.

We are now ready to compute the diffracted power. We start with the Sommerfeld case. The differential area element is $dA = dz d\rho$ where $\rho = x - 100$ cm in Figure 1. Now $\rho = r \cos(\alpha)$ so $d\rho = |r \sin(\alpha) d\alpha|$. Our equation becomes

$$c\epsilon_0 u_d^* u_d \Delta z = \frac{1}{k_s} \int_0^{\pi/2} \frac{c\epsilon_0 \eta^2 T_g}{r \Delta h} \sin(\alpha) f_s^2(\phi, \alpha) dA = \frac{c\epsilon_0 \eta^2 T_g \Delta z}{\Delta h k_s} \int_0^{\pi/2} \sin^2(\alpha) f_s^2(\phi, \alpha) d\alpha. \quad (9)$$

The diffracted intensity in W/m² along the same ray is $c\epsilon_0 u_d^* u_d \Delta z = c\epsilon_0 \eta^2 T_d \Delta z / \Delta h$. We then find

$$T_d = \frac{T_g}{k_s} \int_0^{\pi/2} \sin^2(\alpha) f_s^2(\phi, \alpha) d\alpha. \quad (10)$$

The equation simply says, take T_g and multiply by the geometric factors that enter in the diffraction equation. This is convenient because the power in a single mode that enters our antenna is $k_B T_d \Delta \nu$.

For the case of a round-ended screen we replace $f_s^2(\phi, \alpha)$ by $f(\theta_s, ka)$. The integral is more involved but because $ka \gg 1$ we need only consider $m = 0$ as demonstrated above.

Table 3: The GTD factors for 92 and 151 GHz with a=10 cm

Case	q_0	$a\alpha_0$	$k^{1/2} D_0^2$	$a\alpha_0$	$k^{1/2} D_0^2$
		$a = 0.10$ m 89.5 GHz	$ka = 187.4$ 89.5 GHz	$a = 0.10$ m 146 GHz	$ka = 305.3$ 146 GHz
$u = 0$	3.37213	9.197- <i>i</i> 5.310	3.560+ <i>i</i> 0.954	10.823 - <i>i</i> 6.248	4.189 + <i>i</i> 1.122
$\partial u / \partial n = 0$	1.46935	4.007- <i>i</i> 2.314	5.987+ <i>i</i> 1.604	4.716 - <i>i</i> 2.723	7.046 + <i>i</i> 1.888

Referring to Table² 3, for 146 GHz, the equations for Cases I and II become:

$$\text{Case I} \quad T_d = \frac{T_g}{ks} \int \sin^2(\alpha) |(4.189 + i1.122)e^{(i304-10.823+i6.248)\theta_s(\phi,\alpha)}|^2 d\alpha \quad \text{and} \quad (11)$$

$$\text{Case II} \quad T_d = \frac{T_g}{ks} \int \sin^2(\alpha) |(7.046 + i1.888)e^{(i304-4.716+i2.723)\theta_s(\phi,\alpha)}|^2 d\alpha. \quad (12)$$

One must do the calculations with the complex quantities and then take the magnitude at the end. Note that at longer wavelengths the integrand changes. This is not the case for Sommerfeld diffraction. The rounded edge becomes less effective at longer wavelengths.

We now show how these results compare. Although the “pure Sommerfeld” case, $f_s(\phi, \alpha)^2$ alone, is not applicable it is a useful benchmark and should be an upper limit. In the following we consider various aspects of Equations 10, 11 and 12 but without multiplying by T_g/kr .

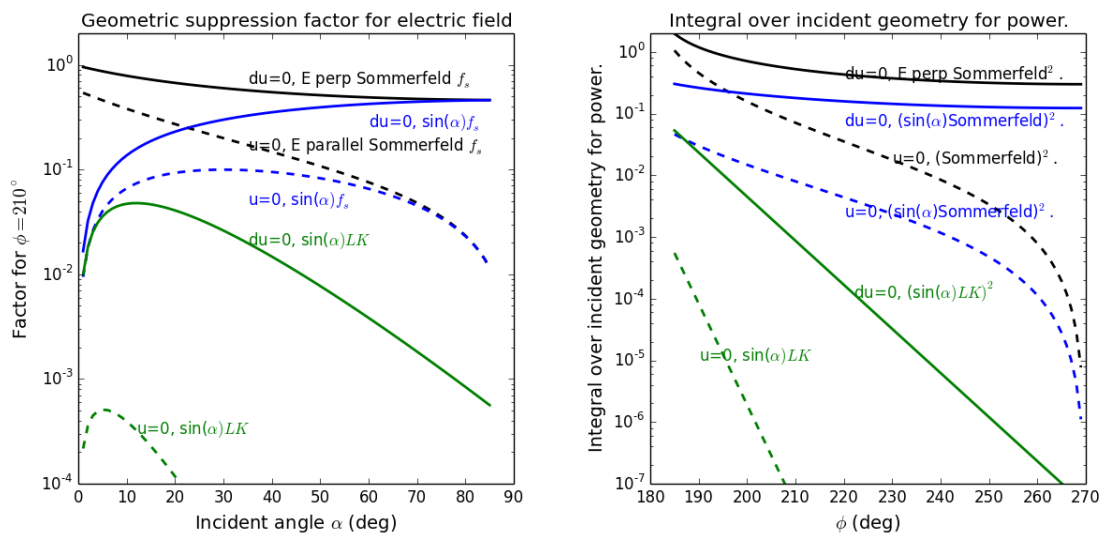


Figure 3: *Left*: The geometric suppression of the field as a function of incident angle. The solid lines show the case for E perpendicular to the edge; the dashed lines are for E parallel. Black is for the straight Sommerfeld case (Equation 1); the blue line is is for Sommerfeld case multiplied by $\sin(\alpha)$ to account for the incident geometry; and green is for the Levy-Keller equation for $a=10\text{cm}$. and multiplied by $\sin(\alpha)$. *Right*: The same cases but now the integral of α is included and we consider the suppression of the total diffracted power as a function of the angle to the ground screen top from the receiver. Neither plot include the factor of $1/\sqrt{rk}$.

Figure 3 shows the effects of geometry on the diffracted radiation. On the left we show the contributions as a function of incident angle for $\phi = 210^\circ$, or a ground screen whose top is at an angle of 30° relative to the receiver entrance. The curves we show are the square root of the integrand in Equations 10, 11 and 12 and thus are proportional to the electric

²In this document precise values are given so that the code can be checked. In the plotting we are a little more relaxed and do not distinguish between, say, 90 and 89 GHz.

field. The pure Sommerfeld case is for reference only. If we had done this for $\phi = 225^\circ$, the black lines would have intercepted the y-axis at 0.74 ($du=0$) and 0.3 ($u=0$) and match the horizontal dashed lined in Figure 2. The $\sin(\alpha)$ factor really only enters when we consider the power, where it enters as $\sin(\alpha)^2$, but we include it here to make the comparison more straightforward. Note that when the edge is rounded, the green lines, most of the power that gets diffracted comes in from shallow angles. This make sense as the other rays shed power as they diffract around the curve. For the knife edge case (blue), most of the power comes in between 20° and 60° .

The right side of the figure shows the same cases but now for the total power. To get the effective temperature, one multiplies by $T_g = 270$ K and divides by kr . There are a couple things of note. In the pure Sommerfeld case (black) the suppression factor appease to go above unity for $\phi = 180^\circ$. This is OK. We need to remember that this is near $\alpha + \phi = \pi$ where the solution breaks down. Also we have not yet divided by k . One of the surprises is that the $du = 0$ blue line is so flat. The diffracted power is not that dependent on ϕ in the Sommerfeld case. The more relevant line is the solid green one in which there is a strong dependence.

We now scan over the design space of distance to the top of the screen vs angle to the top of the screen for a receiver sitting inside a ground screen. The next set of four plots show contour levels for Equation 10 and Equations 11 & 12 for 90 and 150 GHz.

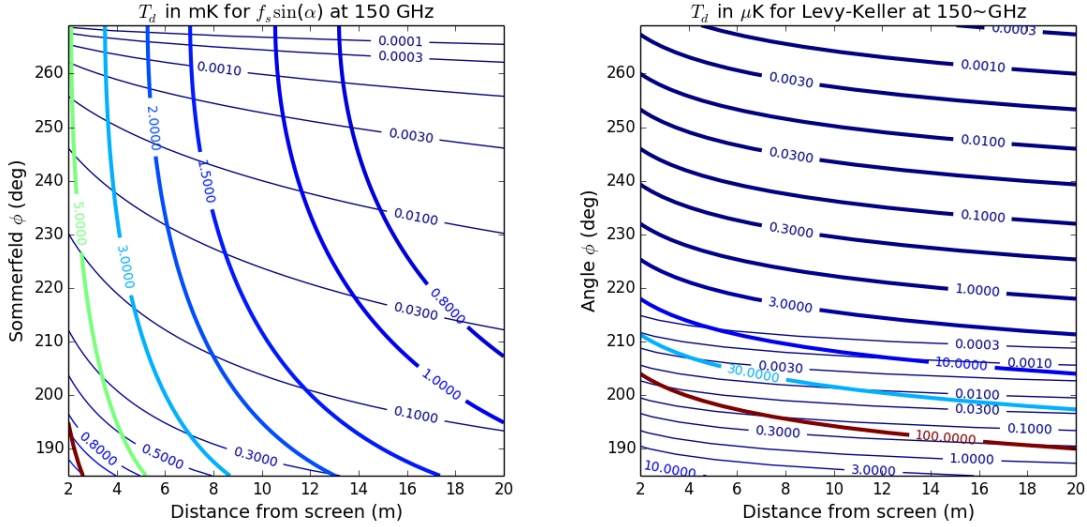


Figure 4: *Left:* The Sommerfeld case, Equation 10, for 150 GHz. The thin lines are for Case I, $u = 0$. The think lines are for Case II, $\partial u/\partial n = 0$. *Right:* The same but for the Levy-Keller case. Note the units here are in μK in contrast to mK.

To connect with right side of Figure 3, we see that for the Sommerfeld case for Case II, the blue line, the value levels off at roughly 0.2. Let's say the top of the screen is 10 m away at an angle of 30° . The diffracted temperature is $0.2T_g/kr = 1.7\text{mK}$ where we have taken $T_g = 270$ K and $k = 3141 \text{ m}^{-1}$ for 150 GHz. This is close to the value for coordinates $x = 10$ m and $y = 210^\circ$.

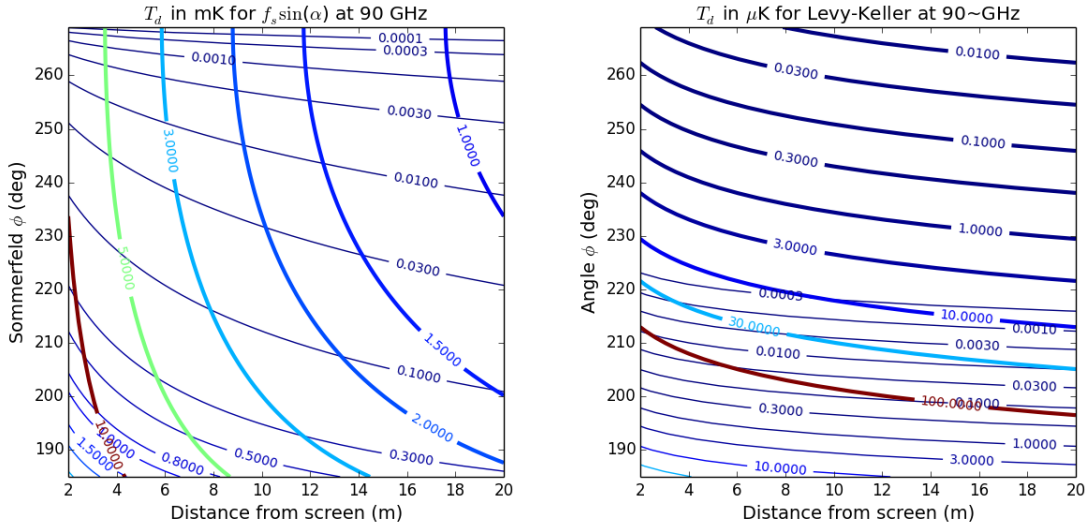


Figure 5: *Left:* The Sommerfeld case, Equation 10, for 90 GHz. The thin lines are for Case I, $u = 0$. The thick lines are for Case II, $\partial u / \partial n = 0$. These contours are the same as for the left side of the previous figure but multiplied by $150/90$. *Right:* The same but for the Levy-Keller case. Note again that the units here are in μK in contrast to mK.

References

- [1] M. Born and E. Wolf. *Principles of Optics*. Pergamon Press, Oxford, England, sixth edition, 1980.
- [2] J. Keller. Diffraction of a convex cylinder. *IEEE Transactions on Antennas and Propagation*, 4:312–321, July 1956.
- [3] J. B. Keller. How Dark is the Shadow of a Round-Ended Screen? *Journal of Applied Physics*, 30:1452–1454, September 1959.
- [4] J. B. Keller. Geometrical theory of diffraction. *Journal of the Optical Society of America (1917-1983)*, 52:116, February 1962.
- [5] J. B. Levy, B. R. Keller. Diffraction by a Smooth Object. *Communications on Pure and Applied Mathematics*, pages 159–209, February 1959.
- [6] L. Page, C. Jackson, C. Barnes, C. Bennett, M. Halpern, G. Hinshaw, N. Jarosik, A. Kogut, M. Limon, S. S. Meyer, D. N. Spergel, G. S. Tucker, D. T. Wilkinson, E. Wollock, and E. L. Wright. The Optical Design and Characterization of the Microwave Anisotropy Probe. *Ap. J.*, 585:566–586, March 2003.